NISER

Integrated Physics Lab

P441

Metamaterial hyperlens demonstration of propagation without diffraction

Author :
Abhishek (1911007)

November 29th, 2022

Metamaterial hyperlens demonstration of propagation without diffraction

Abhishek
School of Physical Sciences, National Institute of Science Education and Research, HBNI, Jatni-752050, India.
(*abhishek.2019@niser.ac.in)
(Dated: November 29, 2022)

In this experiment, we created hyperlens for microwaves in which microwaves can propagate without diffraction. It was made by using the conducting wires arrays. We used ribbon cables that were readily available and cost significantly less. Details of the construction of this material are given in the following sections. This material has extreme anisotropy, appearing metallic to longitudinally polarized fields and dielectric to transversely polarized fields. Using this metamaterial, we successfully demonstrated diffraction-free propagation.

I. INTRODUCTION

Metamaterials are currently a topic of intense research because they have extraordinary properties, such as a negative refractive index, and can be used to fabricate devices with functionalities inaccessible to traditional materials.The concept was first introduced by Veselago in 1968 [7] which theoretically investigated the electrodynamic consequences of a medium having both ε and μ negative and concluded that such a medium would have dramatically different propagation characteristics stemming from the sign change of the group velocity, including reversal of both the Doppler shift and Cherenkov radiation, anomalous refraction, and even reversal of radiation pressure to radiation tensionNegative ε and μ gives rise to negative refractive index materials which can exhibit exotic and unique electromagnetic properties not inherent in the individual constituent components Some potential functionalities, such as invisibility cloaking, have received widespread publicity. As a result, there is a general interest in metamaterials, which creates an opportunity to engage students in "research-led" learning about some exciting physics. Metamaterials have a sub-wavelength structure, a composite of two substantially different materials, typically a metal and a dielectric. They derive their properties primarily from the geometry of their structure rather than their constituent materials. For instance, the permittivity value can be engineered with a metamaterial comprised of a regular array of fine wires in a dielectric. The permeability can be arranged with a similar structure but using split rings rather than wire cables.

A periodic array of conducting elements can be an effective medium for EM wave scattering when the wavelength is much longer than the element dimension and lattice spacing. What makes the resulting media special is that the effective permittivity' effective and permeability μ_{eff} can have values not observed in ordinary materials. An example medium is a three-dimensional array of intersecting thin straight wire. Many exciting properties, including a negative refractive index, invisibility, and cloaking, are possible with metamaterials. In this work, we focus on hyperlensing, primarily for experimental practicality, the potential for real-world application, and the accessibility of the physical concepts at the undergraduate level. A hyperlens permits imaging of detail smaller than $\frac{\lambda}{2}$, which is usually impossible as this is below the diffraction limit.

II. THEORY

A. Near-field information and the diffraction limit

lets consider a planar object on the $z = 0$ plane and the optical axis for imaging along the z axis as shown in figure 24. Let $\boldsymbol{E}(x,y,0)$ be the associated electric field. Now the electromagnetic fields over all space can be written down as

$$\boldsymbol{E}(x,y,z;t) = \left(\frac{1}{2\pi}\right)^2 \int_{k_x}\int_{k_y} \mathrm{d}k_x\,\mathrm{d}k_y \mathscr{E}(k_x,k_y)\exp\left[\mathrm{i}\left(k_x x + k_y y + k_z z - \omega t\right)\right]$$

where ω is the frequency of the radiation and

$$\mathscr{E}(k_x,k_y) = \int_x\int_y \mathrm{d}x\,\mathrm{d}y \boldsymbol{E}(x,y,0)\exp\left[-\mathrm{i}\left(k_x x + k_y y\right)\right]$$

is the Fourier transform of the spatial variation of the source. The Maxwell equations impose the condition that

$$k_x^2 + k_y^2 + k_z^2 = \varepsilon_0\mu_0\frac{\omega^2}{c^2} = k_0^2$$

in free space. Note that k_x and k_y represent the Fourier components of the spatial variation in the source in the corresponding directions.

Now $k_x = 2\pi/\Delta_x$ and $k_y = 2\pi/\Delta_y$, where Δ_x and Δ_y are some spatial periods of the variation. The source can have intensity or field variations over arbitrarily small distances. There is no restriction on that. As an example, consider the case of isolated molecules on a surface emitting radiation, in which case the $\Delta_{x,y}$ can literally be on atomic length-scales. The corresponding transverse wave-vectors k_x and k_y will then be very large, in which case the dispersion equation, equation (4.3), cannot be satisfied without making the associated k_z imaginary. Thus the waves with large $k_x > k_0$ and $k_y > k_0$ are evanescent and decay in amplitude exponentially away from the source $z = 0$ plane.

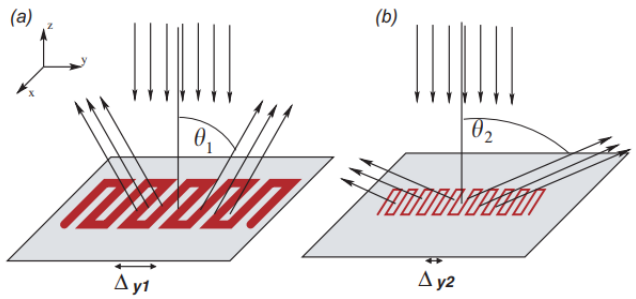

FIG. 1: Radiation is scattered and emitted by an object. The angle at which light comes out depends on the spatial features of the source. A periodic object with large spatial period scatters the light through small angles (a), while the light comes out at large angles for a periodic object with small spatial periods (b)

B. Dispersion relation Derivation

Propagation of EM plane waves in materials at fixed frequencies of the wave vector causes the dispersion surfaces. For our theoretical wave propagation analysis, we choose an optic axis in the direction of the unit vector $\hat{\imath}$. Then, we calculate the dispersion relations and discuss the issue for both cases of dissipative and non-dissipative mediums. To simplify the analysis, we assume a linear material with permittivity $\underline{\underline{\varepsilon}}$ and permeability $\underline{\underline{\mu}}$ tensors which are simultaneously diagonalizable. i.e.

$$\underline{\underline{\varepsilon}} = \begin{bmatrix} \varepsilon_{\parallel} & 0 & 0 \\ 0 & \varepsilon_{\perp} & 0 \\ 0 & 0 & \varepsilon_{\perp} \end{bmatrix} \quad \text{and} \quad \underline{\underline{\mu}} = \begin{bmatrix} \mu_{\parallel} & 0 & 0 \\ 0 & \mu_{\perp} & 0 \\ 0 & 0 & \mu_{\perp} \end{bmatrix}$$

where $\varepsilon_{\parallel}$and $\mu_{\parallel}$are the elements of permittivity and permeability tensors along the optic axis, and $\varepsilon_{\perp}$ and $\mu_{\perp}$ are the elements of the two tensors in the plane perpendicular to the optic axis, respectively. For non-dissipative mediums, elements of these two tensors are real, whereas, for dissipative ones, they are complex-valued. The real parts of these scalars are positive for natural mediums, but they can have any sign for metamaterials. There is no fundamental objection to the real parts of the ε and μ being negative. The dispersion equation for plane waves in such mediums leads to the propagation of two different types of linearly polarized waves, called magnetic and electric modes. The electric and magnetic waves are

$$\boldsymbol{E}(\boldsymbol{r}) = \boldsymbol{E}_0 e^{i\boldsymbol{K}.\boldsymbol{r}}$$
$$\boldsymbol{H}(\boldsymbol{r}) = \boldsymbol{H}_0 e^{i\boldsymbol{K}.\boldsymbol{r}}$$

where K wave vector is defined in the most general form

$$\boldsymbol{K} = \alpha\hat{\imath} + \beta\hat{k}$$

where $\alpha \in \mathrm{R}, \beta \in \mathrm{C}$ and $\hat{k}$ is the unit vector directed along the z axis . This form of k is appropriate for planar boundary value problems and from the practical viewpoint of potential optical devices. We note that the plane waves (2) are generally non-uniform. So the form of the electric field will be as follows.

$$\boldsymbol{E}(\boldsymbol{r}) = \boldsymbol{E_0} e^{i\alpha x} e^{i\mathrm{Re}\{\beta\}z} e^{-\mathrm{Im}\{\beta\}z}$$

$$\nabla \times \boldsymbol{E}(\mathbf{r}) = i\omega \underline{\underline{\mu}} \boldsymbol{H} =$$
$$\nabla \times \boldsymbol{H}(\mathbf{r}) = -i\omega \underline{\underline{\varepsilon}} \boldsymbol{E}(\mathbf{r})$$

5 Combining (5) and (6) we have

$$\nabla \times \nabla \times \boldsymbol{E}(\mathbf{r}) = i\omega^2 \underline{\underline{\mu}} \nabla \times \boldsymbol{H}(\mathbf{r})$$

which yields the vector Helmholtz equation

$$\nabla \times \nabla \times \boldsymbol{E}(\mathbf{r}) = \omega^2 \underline{\underline{\mu}}\,\underline{\underline{\varepsilon}} \boldsymbol{E}(\mathbf{r})$$

The left side of equation (8) can be expressed as

$$\boldsymbol{\nabla} \times \boldsymbol{\nabla} \times \boldsymbol{E}(\mathbf{r}) = \begin{vmatrix} \hat{\imath} & \hat{} & \hat{k} \\ \frac{\partial}{\partial \mathrm{x}} & \frac{\partial}{\partial \mathrm{y}} & \frac{\partial}{\partial \mathrm{z}} \\ \frac{\partial}{\partial \mathrm{y}} E_z - \frac{\partial}{\partial \mathrm{z}} E_y & \frac{\partial}{\partial \mathrm{z}} E_x - \frac{\partial}{\partial \mathrm{x}} E_z & \frac{\partial}{\partial \mathrm{x}} E_y - \frac{\partial}{\partial \mathrm{y}} E_x \end{vmatrix}$$

Hence

$$\begin{aligned} \boldsymbol{\nabla} \times \boldsymbol{\nabla} \times \boldsymbol{E}(\mathbf{r}) = & \left(\frac{\partial}{\partial \mathrm{y}} \left\{ \frac{\partial}{\partial \mathrm{x}} E_y - \frac{\partial}{\partial \mathrm{y}} E_x \right\} - \frac{\partial}{\partial \mathrm{z}} \left\{ \frac{\partial}{\partial \mathrm{z}} E_x - \frac{\partial}{\partial \mathrm{x}} E_z \right\} \right) \hat{\imath} \\ & - \left(\frac{\partial}{\partial \mathrm{x}} \left\{ \frac{\partial}{\partial \mathrm{x}} E_y - \frac{\partial}{\partial \mathrm{y}} E_x \right\} - \frac{\partial}{\partial \mathrm{z}} \left\{ \frac{\partial}{\partial \mathrm{y}} E_z - \frac{\partial}{\partial \mathrm{z}} E_y \right\} \right) \hat{} \\ & + \left(\frac{\partial}{\partial \mathrm{x}} \left\{ \frac{\partial}{\partial \mathrm{z}} E_x - \frac{\partial}{\partial \mathrm{x}} E_z \right\} - \frac{\partial}{\partial \mathrm{y}} \left\{ \frac{\partial}{\partial \mathrm{y}} E_z - \frac{\partial}{\partial \mathrm{z}} E_y \right\} \right) \hat{\mathrm{k}} \end{aligned}$$

So we have

$$\begin{aligned} \boldsymbol{\nabla} \times \boldsymbol{\nabla} \times \boldsymbol{E}(\mathbf{r}) = & \left(\left\{ \frac{\partial^2}{\partial \mathrm{yx}} E_y - \frac{\partial^2}{\partial \mathrm{yy}} E_x \right\} - \left\{ \frac{\partial^2}{\partial zz} E_x - \frac{\partial^2}{\partial \mathrm{zx}} E_z \right\} \right) \hat{\imath} \\ & - \left(\left\{ \frac{\partial^2}{\partial \mathrm{xx}} E_y - \frac{\partial^2}{\partial \mathrm{xy}} E_x \right\} - \left\{ \frac{\partial^2}{\partial \mathrm{zy}} E_z - \frac{\partial^2}{\partial \mathrm{zz}} E_y \right\} \right) \hat{\mathrm{j}} \\ & + \left(\left\{ \frac{\partial^2}{\partial \mathrm{xz}} E_x - \frac{\partial^2}{\partial \mathrm{xx}} E_z \right\} - \left\{ \frac{\partial^2}{\partial \mathrm{yy}} E_z - \frac{\partial^2}{\partial \mathrm{yz}} E_y \right\} \right) \hat{\mathrm{k}} \end{aligned}$$

10 Note that in the above equation, the y component is zero, therefore the left side of equation (8) will be

$$\boldsymbol{\nabla} \times \boldsymbol{\nabla} \times \boldsymbol{E}(\mathbf{r}) = \left(\frac{\partial^2}{\partial \mathrm{zx}} E_z - \frac{\partial^2}{\partial zz} E_x \right) \hat{\imath} + \left(\left\{ \frac{\partial^2}{\partial \mathrm{xz}} E_x - \frac{\partial^2}{\partial \mathrm{xx}} E_z \right\} \right) \hat{\mathrm{k}}$$

In the following we consider Gauss's law for neutral medium

$$\nabla \cdot D = 0$$

13 So equation (12) can be written as

$$\nabla \times \nabla \times \boldsymbol{E}(\mathbf{r}) = -\left(\frac{\partial^2}{\partial z^2} + \frac{\varepsilon_{\parallel}}{\varepsilon} \frac{\partial^2}{\partial \mathrm{x}^2} \right) E_x \hat{\mathrm{i}} - \left(\frac{\partial^2}{\partial \mathrm{x}^2} + \frac{\varepsilon}{\varepsilon_{\parallel}} \frac{\partial^2}{\partial z^2} \right) E_z \hat{\mathrm{k}}$$

The right side of equation (8) will be expressed as follows

$$\omega^2 \underline{\underline{\mu}}\,\underline{\underline{\varepsilon}} \boldsymbol{E}(\mathbf{r}) = \omega^2 \begin{bmatrix} \varepsilon_x & 0 & 0 \\ 0 & \varepsilon_{\perp} & 0 \\ 0 & 0 & \varepsilon_{\perp} \end{bmatrix} \begin{bmatrix} \mu_{\perp} & 0 & 0 \\ 0 & \mu_{\parallel} & 0 \\ 0 & 0 & \mu_{\perp} \end{bmatrix} \begin{bmatrix} E_x & E_y & E_z \end{bmatrix}$$

Or

$$\omega^2 \underline{\underline{\mu}}\,\underline{\underline{\varepsilon}}\boldsymbol{E}(\mathbf{r}) = \omega^2 \varepsilon_x \mu_\perp E_x \hat{\imath} + \varepsilon_\perp \mu_\perp E_z \hat{\mathrm{K}}$$

By substituting equations (14) and (16) in equation (8), the dispersion equation for the electric field is obtained

$$\varepsilon_\perp \beta^2 + \varepsilon_\parallel \alpha^2 = \omega^2 \varepsilon_\perp \varepsilon_\parallel \mu_\perp$$

Or 17

$$\frac{\beta^2}{\varepsilon_\parallel} + \frac{\alpha^2}{\varepsilon_\perp} = \omega^2 \mu_\perp$$

Analogously, for magnetic modes we have

$$\mu_\parallel \alpha^2 + \mu_\perp \beta^2 = \omega^2 \mu_\parallel \varepsilon_\perp \mu_\perp$$

$$\frac{\beta^2}{\mu_\parallel} + \frac{\alpha^2}{\mu_\perp} = \omega^2 \varepsilon_\perp$$

18 Now we are able to analyze the dispersion equation in dielectric-magnetic mediums by using relations (17) and (18).

C. Modification of ordinary phenomenon in NRMs

1. *"Reversal" of Snell's law*

A Left-Handed medium can be interpreted as having a negative refractive index, n.

$$Sin(\theta_I) = \pm |n| Sin(\theta_T)$$

Hence the snell's law is interpreted as in FIG.2

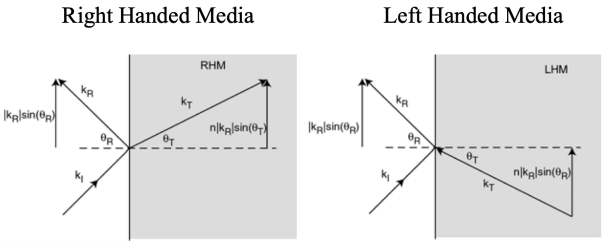

$k_T = nk_I$

FIG. 2: Reversal of Snell's law

2. *Inverse Doppler effect*

Conventional Doppler shifts occur on reflection of waves propagating in media with normal dispersion from a moving boundary (Fig.3). Inverse Doppler shifts are predicted to occur on reflection of waves propagating in media with anomalous dispersion from a moving boundary (Fig.3).

The difference is that waves in normally dispersive media have group velocity and phase velocity , that are parallel, whereas waves in anomalously dispersive media have group velocity and phase velocity that are antiparallel. For a wave in a normal medium of frequency ω_i in a stationary frame of reference incident on a receding boundary, the boundary velocity and the phase velocity of the incident wave are parallel; therefore, the incident field in the frame of the receding boundary oscillates with a relatively low frequency. Boundary conditions in this case dictate that the frequency of the reflected wave is less than ω_i, as expected for the conventional Doppler effect (Fig.3).

In the anomalously dispersive medium, the phase velocity of the incident wave and the boundary velocity are antiparallel (Fig.3). In this case, the incident field in the frame of the boundary oscillates with a relatively high frequency, and boundary conditions dictate that the frequency of the reflected wave is greater than ω_i, as expected for the inverse Doppler effect.

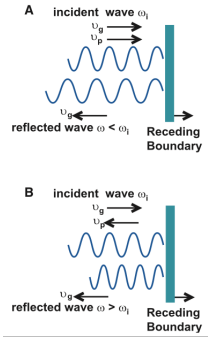

FIG. 3: Reflection of waves from a receding boundary

D. Negative dielectric materials

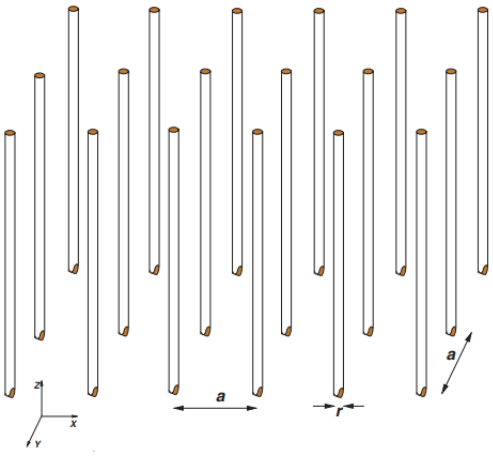

FIG. 4: An array of infinitely long thin metal wires of radius r and a lattice period of a behaves as a low frequency plasma for the electric field oriented along the wires.

The effective electron density is immediately seen to be

$$n_{\text{eff}} = \frac{\pi r^2}{a^2} n,$$

where n is the actual density of conduction electrons in the metal. There is a second equally important effect to be considered. The thin wires have a large inductance, and it is not easy to change the currents flowing in these wires. Thus, it appears that the charge carriers, namely the electrons, have acquired a tremendously large mass. To see this, consider the magnetic field at a distance ρ from a wire. On average, we can assume a uniform $\boldsymbol{D}$ field within the unit cell. But the current density is not uniform, leading to a non-zero non-uniform magnetic field that is large and close to the wires, which contributes to most of the flux. By symmetry, there is a point of zero fields in between the wires, and hence we can estimate the magnetic field along the line between two wires as

$$\boldsymbol{H}(\rho) = \frac{\hat{\phi} I}{2\pi} \left(\frac{1}{\rho} - \frac{1}{a-\rho} \right).$$

The vector potential associated with the field of a single infinitely long current-carrying conductor is non-unique unless the boundary conditions are specified at definite points. In our case, we have a periodic medium that sets a critical length of $a/2$. We can assume that the vector potential associated with a single wire is

$$\begin{aligned} \boldsymbol{A}(\rho) &= \tfrac{\hat{z} I}{2\pi} \ln \left[\tfrac{a^2}{4\rho(a-\rho)} \right] \quad \forall \rho < \tfrac{a}{2}, \\ &= 0 \quad \forall \rho > \tfrac{a}{2}. \end{aligned}$$

This choice avoids the vector potential of one wire overlapping with another wire and thus the mutual induction between the adjacent wires is addressed to some extent. Noting that $r \ll a$

by about three orders of magnitude in our model and that the current $I = \pi r^2 nev$, where v is the mean electron velocity, we can write the vector potential as

$$\boldsymbol{A}(\rho) = \frac{\mu_0 \pi r^2 nev}{2\pi} \ln \left(\frac{a}{\rho} \right) \hat{z}.$$

This is a very good approximation of the mean-field limit. We have considered only two wires, and the lattice actually has four-fold symmetry. The actual deviations from this expression are much smaller than in our case. We note that the canonical momentum of an electron in an electromagnetic field is $\boldsymbol{p} + e\boldsymbol{A}$. Thus assuming that the electrons flow on the surface of the wire (assuming a perfect conductor), we can associate a momentum per unit length of the wire of

$$\boldsymbol{p} = \pi r^2 ne \boldsymbol{A}(r) = \frac{\mu_0 \pi^2 r^4 n^2 e^2 v}{2\pi} \ln \left(\frac{a}{r} \right) = m_{\text{eff}} \pi r^2 nv$$

and thus an effective mass of

$$m_{\text{eff}} = \frac{\mu_0 \pi r^2 ne^2}{2\pi} \ln \left(\frac{a}{r} \right),$$

for the electron. Thus, assuming a longitudinal plasmonic mode for the system, we have

$$\omega_{\text{p}} = \frac{n_{\text{eff}} e^2}{\varepsilon_0 m_{\text{eff}}} = \frac{2\pi c^2}{a^2 \ln(a/r)}$$

for the plasmon frequency. We note that a reduced effective electron density and a tremendously increased effective electronic mass would immediately reduce the plasmon frequency for this system. Typically one can choose $r = 1\mu\text{m}, a = 10$ mm and aluminium wires $\left(n = 10^{29}\ \text{m}^{-3}\right)$, which gives an effective mass of

$$m_{\text{eff}} = 2.67 \times 10^{-26}\ \text{kg}$$

that is almost 15 times that of a proton, and a plasma frequency of about 2 GHz! Thus, we have succeeded in obtaining a negative dielectric material at microwave frequencies.

E. Diffraction Without Propagation

The first section discussed a brief theory for Near field and diffraction limit. There we saw that $k_x(2\pi/\Delta_x)$ and $k_y(2\pi/\Delta_y)$ will be very large if we have very small spacing $\Delta_{x,y}$. then the only possible solution for k_z in the dispersion relation (17) that we derived in the previous section will be imaginary and the field is evanescent. However, this constraint can be broken using metamaterial made from wire arrays. Such material consists of a transverse two-dimensional periodic array of longitudinally oriented metal wires embedded in a dielectric. The wire spacing and diameter are substantially smaller than the wavelengths with which it will interact; hence, it can be considered an effective medium. This material has extreme anisotropy, appearing metallic to longitudinally polarized fields and dielectric to transversely polarized fields. Thus, the transverse and longitudinal permittivities have an opposite sign

$$(\varepsilon_t > 0; \varepsilon_z < 0)$$

, and the dispersion relation becomes

$$\frac{k_t^2}{\varepsilon_z} - \frac{|k_z^2|}{|\varepsilon_t|} = \frac{\omega^2}{c^2}$$

; (2) where now there exists a real solution no matter how large k_t. This means all spatial frequencies in the object have propagating solutions, and propagation without diffraction is possible.7 In practice, $|\varepsilon_z| \gg \varepsilon_t$ so that $k_z \approx \sqrt{\varepsilon_t}(\omega/c)$ and all transverse spatial frequencies propagate with approximately the speed of light in the dielectric. Thus, if we can fabricate such a structure, it will carry a field distribution with sub-wavelength features from one transverse face to the other without diffraction.

III. EXPERIMENT DESIGN

- The Source is placed on an a height adjustable jack. The detector is fixed on a travelling microscope equipped with a vernier scale in the y-axis.

- The slits consists of a pair of L shaped metal plates. The slit width is adjusted to some fraction of the wavelength.(2 mm). The slits are covered with aluminium foil on the sides to prevent accidental leakage of the stray microwaves.

- The x and y axis controls are then optimized to maximize reading.

- The transverse offset is measured on the travelling microscope, and the corresponding detector voltage is also noted down.

- The metamaterial is made by alternate close cubical packing of wire ribbons. In our design, we have 12 rows of wire ribbons, each wire ribbon plane containing 40 wires.

- The length of the metamaterial along the propagation direction is 5 cm.

- Data is acquired for far-field, with and without metamaterial. Near field transverse offset could not be acquired due to intense fluctuation of voltmeter. However, we note that the near field signal peaks upto 0.6 V, which is close to the peak obtained by the metamaterial (0.5 V).

FIG. 5: Side, top and front view of a Wire mesh made by ribbon cables stacking.

A. Setup

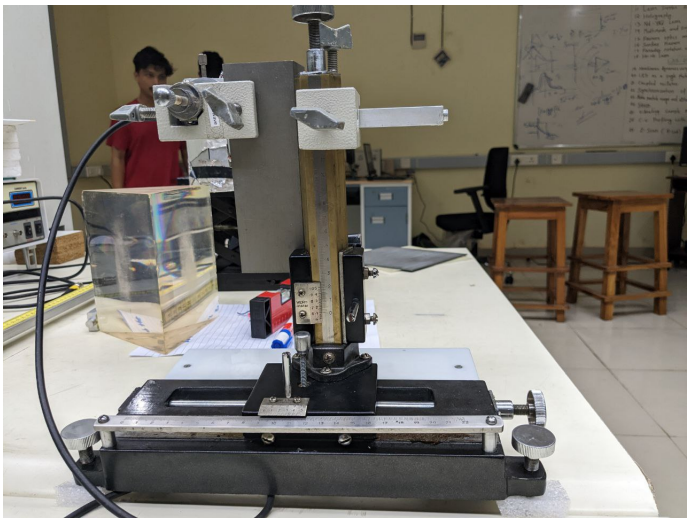

FIG. 7: Detector attached with travelling microscope for measuring transverse offset

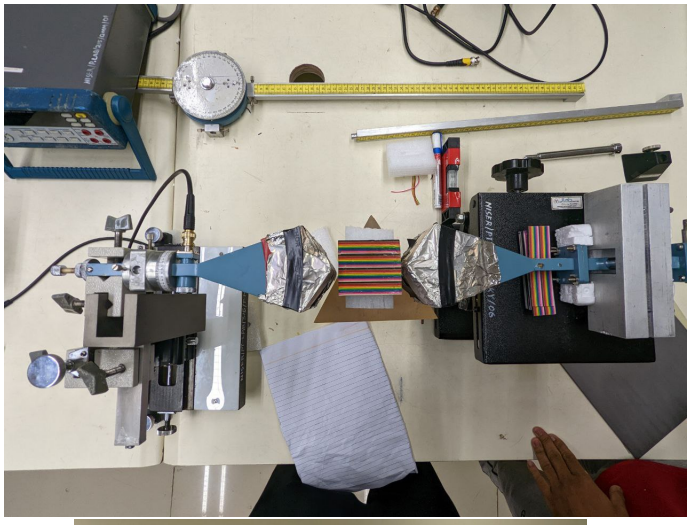

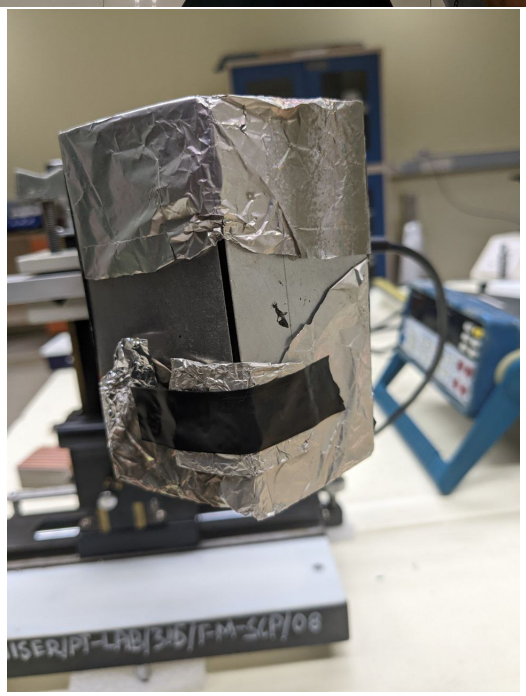

FIG. 6: Top View of the Setup and Slit front view

B. Observed Data

C. Results

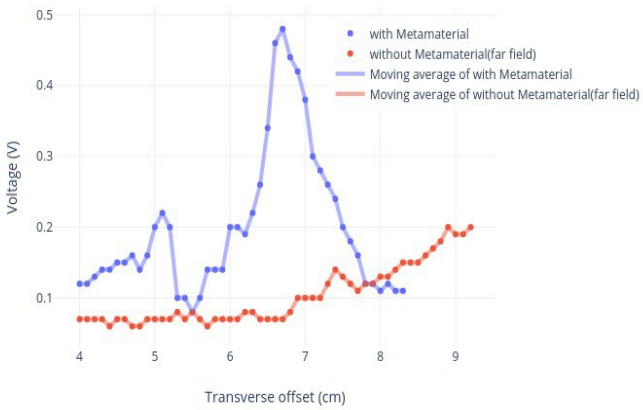

FIG. 9: .

We observe a significant amount of transmission, which (in principle) coincides with near-field transverse offset. Note that near-field offset could not be plotted due to intense fluctuation of voltmeter reading at near field (possibly due to more sensitivity to minor fluctuation in slit width).

The peak obtained at near-field transmission was 0.6 V, which is close to the peak of the far-field with metamaterial. Far-field transverse offset remains relatively low, re-enforcing our claim of disperisonless transmission of microwaves.
Fig 9 are the dispersion plots of the above curve.

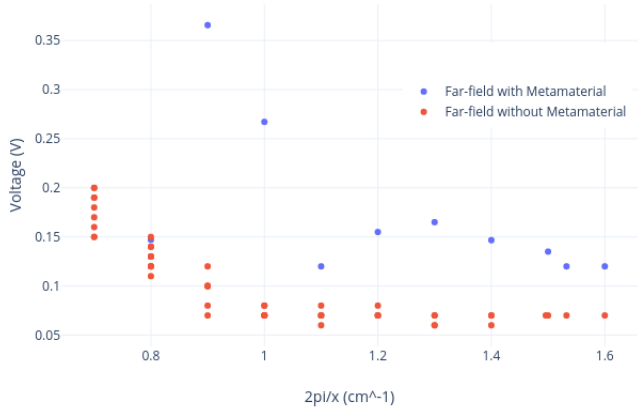

FIG. 10: Dispersion relation for far-field, with and without metamaterial.

D. Conclusion

In conclusion, we have demonstrated dispersionless transmission across the metamaterial over the far-field transmission of microwaves (2.85 GHz). The metamaterial is based on a wire lattice design.
The peak transmission through the metamaterial is close to the near field peak value (0.6 V).
Such NRMs have many interesting prospective including near field imaging, super-lenses and so on. The imaging resolution of conventional lenses is limited by diffraction. Artificially engineered metamaterials allow the possibility of building a super-lens that overcomes this limit. The following figure represents the object (above) and its respective near-field image (below) formed by a super-lens operating 395 nm.
Also the experiment gives an insight about the interplay between group velocity and phase velocity in a medium. Laws of nature permits the existence of left handed materials. The relation between v_g and v_p in left handed mediums give rise to counter-intuitive phenomenon such as *reverse Snell's law, inverse Doppler effect* and so on.

FIG. 11: object and near-field image formed by super-lens

IV. PRECAUTIONS

1. Make sure all the components are connected properly.
2. Do not disturb the setup while taking the measurements.

V. REFERENCES

- https://dsl.nju.edu.cn/litao/res/meta%20review/%5BRPP2005%5D%20Physics%20of%20negative%20refractive%20index%20materials.pdf
- https://journals.aps.org/prl/pdf/10.1103/PhysRevLett.85.3966

Table 1

1st data with mm		2nd data with mm			1st data without mm		
Distance (cm)	Voltage (V)	Distance (cm)	1/V	Voltage (V)	Distance (cm)	1/V	Voltage (V)
3.8	0.07	4	8.33333333333333	0.12	4	14.2857142857143	0.07
3.9	0.07	4.1	8.33333333333333	0.12	4.1	14.2857142857143	0.07
4	0.07	4.2	7.69230769230769	0.13	4.2	14.2857142857143	0.07
4.1	0.07	4.3	7.14285714285714	0.14	4.3	14.2857142857143	0.07
4.2	0.08	4.4	7.14285714285714	0.14	4.4	16.6666666666667	0.06
4.3	0.09	4.5	6.66666666666667	0.15	4.5	14.2857142857143	0.07
4.4	0.1	4.6	6.66666666666667	0.15	4.6	14.2857142857143	0.07
4.5	0.1	4.7	6.25	0.16	4.7	16.6666666666667	0.06
4.6	0.1	4.8	7.14285714285714	0.14	4.8	16.6666666666667	0.06
4.7	0.09	4.9	6.25	0.16	4.9	14.2857142857143	0.07
4.8	0.08	5	5	0.2	5	14.2857142857143	0.07
4.9	0.07	5.1	4.54545454545455	0.22	5.1	14.2857142857143	0.07
5	0.07	5.2	5	0.2	5.2	14.2857142857143	0.07
5.1	0.07	5.3	10	0.1	5.3	12.5	0.08
5.2	0.08	5.4	10	0.1	5.4	14.2857142857143	0.07
5.3	0.08	5.5	12.5	0.08	5.5	12.5	0.08
5.4	0.08	5.6	10	0.1	5.6	14.2857142857143	0.07
5.5	0.08	5.7	7.14285714285714	0.14	5.7	16.6666666666667	0.06
5.6	0.09	5.8	7.14285714285714	0.14	5.8	14.2857142857143	0.07
5.7	0.1	5.9	7.14285714285714	0.14	5.9	14.2857142857143	0.07
5.8	0.11	6	5	0.2	6	14.2857142857143	0.07
5.9	0.12	6.1	5	0.2	6.1	14.2857142857143	0.07
6	0.11	6.2	5.26315789473684	0.19	6.2	12.5	0.08
6.1	0.11	6.3	4.54545454545455	0.22	6.3	12.5	0.08
6.2	0.12	6.4	3.84615384615385	0.26	6.4	14.2857142857143	0.07
6.3	0.12	6.5	2.94117647058824	0.34	6.5	14.2857142857143	0.07
6.4	0.11	6.6	2.17391304347826	0.46	6.6	14.2857142857143	0.07
6.5	0.14	6.7	2.08333333333333	0.48	6.7	14.2857142857143	0.07
6.6	0.17	6.8	2.27272727272727	0.44	6.8	12.5	0.08
6.7	0.19	6.9	2.38095238095238	0.42	6.9	10	0.1
6.8	0.21	7	2.63157894736842	0.38	7	10	0.1
6.9	0.2	7.1	3.33333333333333	0.3	7.1	10	0.1
7	0.17	7.2	3.57142857142857	0.28	7.2	10	0.1
7.1	0.14	7.3	3.84615384615385	0.26	7.3	8.33333333333333	0.12
7.2	0.13	7.4	4.16666666666667	0.24	7.4	7.14285714285714	0.14
7.3	0.11	7.5	5	0.2	7.5	7.69230769230769	0.13
7.4	0.1	7.6	5.55555555555556	0.18	7.6	8.33333333333333	0.12
7.5	0.09	7.7	6.25	0.16	7.7	9.09090909090909	0.11
7.6	0.08	7.8	8.33333333333333	0.12	7.8	8.33333333333333	0.12
7.7	0.08	7.9	8.33333333333333	0.12	7.9	8.33333333333333	0.12
7.8	0.09	8	9.09090909090909	0.11	8	7.69230769230769	0.13
7.9	0.1	8.1	8.33333333333333	0.12	8.1	7.69230769230769	0.13
8	0.12	8.2	9.09090909090909	0.11	8.2	7.14285714285714	0.14
8.1	0.12	8.3	9.09090909090909	0.11	8.3	6.66666666666667	0.15
8.2	0.11	8.4			8.4	6.66666666666667	0.15
8.3	0.09	8.5			8.5	6.66666666666667	0.15
8.4	0.09	8.6			8.6	6.25	0.16
8.5	0.1	8.7			8.7	5.88235294117647	0.17
8.6	0.1	8.8			8.8	5.55555555555556	0.18
8.7	0.11	8.9			8.9	5	0.2
8.8	0.12	9			9	5.26315789473684	0.19
8.9	0.12	9.1			9.1	5.26315789473684	0.19
9		9.2			9.2	5	0.2

- https://journals.aps.org/prl/pdf/10.1103/PhysRevLett.84.4184
- https://en.wikipedia.org/wiki/Superlens
- https://arxiv.org/pdf/0807.4915.pdf
- https://doi.org/10.1070/PU1968v010n04ABEH003699
- https://journals.aps.org/prl/abstract/10.1103/PhysRevLett.76.4773
- Calculation of dispersion equations for uniaxial dielectric-magnetic https://arxiv.org/pdf/1702.08765.pdf

VI. ACKNOWLEDGEMENT

I would like to thank Dr.Santosh Babu Gunda and Dr. Ritwick Das for their guidance during the course of experiment. Also I would like to acknowledge the Niser Workshop for providing with the custom slit design of the horn antenna.